WILEY

Cladistics

Cladistics (2025) 1–17

doi: 10.1111/cla.70015

The evolutionary history of Rhinocerotidae: phylogenetic insights and climate influences

Antonio Borrani[a], Paweł Mackiewicz*[b,*], Oleksandr Kovalchuk[c,d,e], Zoltán Barkaszi[c,f], Chiara Capalbo[g], Anastasiia Dubikovska[e,h], Urszula Ratajczak-Skrzatek[d], Maxim Sinitsa[i], Krzysztof Stefaniak[d] and Paul P.A. Mazza[g]

[a]*Soprintendenza Archeologia, Belle Arti e Paesaggio per le Province di Frosinone e Latina, Latina, Italy;* [b]*Faculty of Biotechnology, University of Wrocław, Wrocław, Poland;* [c]*National Museum of Natural History, National Academy of Sciences of Ukraine, Kyiv, Ukraine;* [d]*Faculty of Biological Sciences, University of Wrocław, Wrocław, Poland;* [e]*A.S. Makarenko Sumy State Pedagogical University, Sumy, Ukraine;* [f]*John von Neumann University, Kecskemét, Hungary;* [g]*Department of Earth Sciences, University of Florence, Florence, Italy;* [h]*I.I. Schmalhausen Institute of Zoology, National Academy of Sciences of Ukraine, Kyiv, Ukraine;* [i]*Università Roma Tre, Rome, Italy*

Received 5 May 2025; Revised 30 September 2025; Accepted 9 October 2025

Abstract

Family Rhinoceroidae exhibits a complex and debated phylogeny, with fossil records spanning over 50 million years. This study presents a comprehensive phylogenetic total-evidence analysis of Rhinocerotidae to date, integrating morphological, molecular, fossil and paleoclimatic data within maximum parsimony, maximum likelihood, Bayesian and time-calibrated frameworks. A matrix of 106 taxa and 534 morphological characters, including 11 newly defined ones, was assembled through systematic revision of previously ambiguous characters. In contrast to earlier studies, a fossil-based outgroup was selected in place of extant *Tapirus* to improve character polarity and reduce topological artefacts associated with distant outgroup choice. The resulting cladograms resolve longstanding conflicts in rhinocerotid systematics and identify many supported clades. Analyses of the studied clades revealed an association between lineage diversification and climatic thresholds, which appear to have mediated ecological turnover and the differential persistence of traits. The application of an integrative total-evidence approach illustrates the role of climatic and ecological filters in shaping the evolutionary trajectories of megafaunal lineages and contributes to broader methodological discussions in phylogenetics. The analytical framework developed provides a comparative model applicable to both extinct and extant taxa, reaffirming the value of rigorous cladistic methods in paleobiology and systematics.

Introduction

Rhinoceroses are on the brink of extinction, their once-diverse lineage within the family Rhinocerotidae now reduced to a single subfamily with a limited geographic range (Heissig, 1973; Groves, 1983). Despite their precarious status today, many species within Rhinocerotidae thrived for over 40 million years, with horns playing a central role in their evolutionary success (Prothero et al., 1989; Prothero and Schoch, 2002). These mammals evolved a wide range of body plans and ecological adaptations, from short-limbed, semi-aquatic taxa such as *Teleoceras*, to large grazing forms like *Ceratotherium* and *Coelodonta* and dwarf browsers such as *Peraceras hessei* and *Teleoceras meridianum* (Prothero, 1998). Horn morphology also varied considerably, including single nasal horns (*Teleoceras*, *Rhinoceros*), single frontal horns (*Elasmotherium*), paired nasal horns (*Diceratherium*, *Menoceras*) and both nasal and frontal horns (*Diceros*, *Dicerorhinus*,

*Corresponding author:
E-mail address: pamac@smorfland.uni.wroc.pl

[Corrections added on 7 November 2025, after first online publication: the article title has been updated in this version.]

Stephanorhinus, *Ceratotherium*, *Coelodonta*). The absence of horns in many extinct taxa suggests that horn loss and gain may have occurred multiple times independently across lineages, potentially as evolutionary responses to varying ecological pressures (Prothero and Schoch, 2002; Fortelius et al., 2003). However, the precise evolutionary pathways and selective forces underlying these morphological transitions remain only partially understood. This morphological and ecological diversity positions Rhinocerotidae as a model clade for studying macroevolutionary responses to climatic and environmental perturbations. As large herbivores, rhinoceroses have acted as key ecosystem engineers, with evolutionary trajectories highly sensitive to long-term environmental fluctuations. Once comprising a diverse and widespread assemblage, rhinocerotids are now restricted to five extant and mostly threatened species, reflecting a deep history of ecological turnover and selective extinction linked to global environmental change (Heissig, 1996; Fortelius et al., 2014; Bai et al., 2020). The group's biogeographic history reflects the interplay between tectonic processes, such as the uplift of mountain ranges and climate changes including global cooling and habitat shifts (Fortelius et al., 2014; Bai et al., 2020).

Initial diversification of rhinoceroses occurred in Eurasia and North America during the Oligocene, followed by a major dispersal event into Africa in the Early Miocene (Prothero et al., 1986; Saarinen, 2019; Bai et al., 2020). These distributional shifts coincided with significant climatic transitions, including global cooling, the expansion of open environments and fluctuations in atmospheric CO_2 (Mudelsee et al., 2014)—factors likely influencing habitat preferences, body size evolution and extinction susceptibility (Fortelius et al., 2014).

Over the past three decades, phylogenetic relationships among rhinocerotids have been extensively reconstructed using morphology-based character matrices and parsimony analyses (e.g. Antoine, 2002; Piras et al., 2010; Deng et al., 2011; Lord et al., 2019). These studies have greatly improved our understanding but have also revealed persistent uncertainty and conflict in certain nodes, especially regarding the interrelationships among subfamilies such as Aceratheriinae, Teleoceratinae and Elasmotheriinae, as well as the placement of enigmatic Eurasian taxa (Kampouridis et al., 2021; Tissier et al., 2021; Lu et al., 2023; Pandolfi and Martino, 2024). Conflicting topologies often result from differences in taxon sampling, character coding and analytical approaches, including the choice and number of outgroups.

While tapirs (Tapiroidea) are widely accepted as the sister group to rhinocerotoids and have been used as outgroups in many studies (e.g. Antoine, 2002; Becker et al., 2013; Lord et al., 2019), relying on a single outgroup taxon may limit phylogenetic resolution and robustness. Increasing outgroup diversity to include other perissodactyl lineages closely related to rhinoceroses could help better root their phylogenies and clarify their evolutionary relationships.

The rhinocerotid fossil record is comparatively rich and well-studied—arguably among the best within Rhinocerotoidea—providing a strong foundation for phylogenetic research (Prothero and Schoch, 2002; Fortelius et al., 2003). Nevertheless, fragmentary remains, morphological convergence and homoplasy complicate character selection and coding, contributing to unresolved phylogenetic inference, systematic ambiguities and conflicting hypotheses (Groves, 1997; McKenna and Bell, 1997; Moodley et al., 2020).

This study addresses these challenges by presenting the most extensive and comprehensive phylogenetic analysis of Rhinocerotidae to date, integrating a detailed morphological matrix with genetic data, fossil-based time calibrations and paleoclimatic reconstructions to resolve longstanding uncertainties. In particular, it clarifies debated nodes within the family and improves outgroup representation. The morphological data were further examined to explore biogeographic dispersal and ecological adaptation within a paleoclimatic framework.

Materials and methods

Notations and terminology

This study follows the cranial and dentognathic notation and terminology established by Guérin (1980), Antoine (2002) and Lacombat (2006). Upper teeth are denoted by capital letters (e.g. M1, M2 and M3), while lower teeth are represented by lowercase letters (e.g. m1, m2 and m3). Deciduous teeth are indicated by a combination of capital and lowercase 'd'. The abbreviations Mc and Mt refer to metacarpal and metatarsal bones, respectively.

For phylogenetic analyses, the following acronyms are used: ML (Maximum Likelihood), BI (Bayesian Inference), BIC (Bayesian Information Criterion), SH-aLRT (Shimodaira-Hasegawa-like approximate likelihood ratio test), BS (Bootstrapping), NNI (Nearest Neighbor Interchange) and MPI (Message Passing Interface). For morphological data analysis, the relevant acronyms include OTU (Operational Taxonomic Unit), MP (Maximum Parsimony), CI (Consistency Index), RI (Retention Index), TL (Tree Length) and TBR (Tree Bisection and Reconnection). For divergence time estimation, the following acronyms are used: BEAST (Bayesian Evolutionary Analysis by Sampling Trees), MK (Lewis MK substitution models), MC (Markov Chain), LogAnalyzer (Log File Analyzer for Bayesian analyses), ESS (Effective Sample Size) and Highest Posterior Density (HPD).

Molecular data analyses

Phylogenetic analyses were conducted using sequences from 37 concatenated mitochondrial protein-coding and RNA genes, as well as noncoding regions, for 12 species. These sequences included 11 extant and 10 extinct rhinoceroses, with four tapirs serving as outgroups (Table S1). Sequence data were retrieved from GenBank

(www.ncbi.nlm.nih.gov) and aligned using the MAFFT L-INS-i algorithm (Katoh and Standley, 2013), running for 1000 iterations. The alignment, consisting of 16 602 base pairs (bp), was manually inspected and refined in JalView (Waterhouse et al., 2009) (Appendix S2).

To determine the most appropriate substitution models, 64 potential partitions were evaluated. These partitions correspond to the three codon positions of each protein-coding gene, as well as separate partitions for RNA genes and noncoding regions. The suitability of separate versus combined substitution models was assessed using ModelFinder (Chernomor et al., 2016; Kalyaanamoorthy et al., 2017) within IQ-TREE, selecting nine substitution models based on BIC.

ML phylogenetic analyses were performed in IQ-TREE 2.3.4 (Nguyen et al., 2015). Branch support was assessed using SH-aLRT with 10 000 replicates, alongside non-parametric BS with 1000 replicates. Tree searching was carried out using the NNI optimisation algorithm, starting from 1000 initial parsimony trees and retaining the top 100 for further refinement.

Bayesian phylogenetic analyses were conducted using MrBayes 3.2.7a (Ronquist et al., 2012), applying the partitioning scheme identified by ModelFinder. Mixed substitution models (Huelsenbeck et al., 2004) were used to explore a broader parameter space, with rate heterogeneity across sites modelled according to ModelFinder results. Two independent runs, each with 64 MCs, were performed, sampling every 100 generations over 30 million generations. To optimize convergence, the chain heating temperature in the Markov chain was set to 0.001 based on preliminary tests. Convergence was assessed based on split frequency (<0.01), and the final posterior consensus tree was derived from the last 8.355 million generations after discarding the burn-in phase. All parameters showed adequate mixing, with ESS values >200 and Potential Scale Reduction Factor (PSRF) close to 1.0.

Phylogenetic analysis was also conducted using PhyloBayes-MPI 1.9 (Lartillot and Philippe, 2004) under the CAT-GTR+Γ model, with parameters inferred directly from the data. Two independent MCs were run for 100 000 generations, sampling every 100 generations. The last 75 000 trees from each chain were used to compute a posterior consensus after confirming convergence (maxdiff <0.1).

A consensus tree incorporating results from ML and BI was generated in IQ-TREE. This consensus tree was used to infer evolutionary relationships and assess the robustness of the recovered clades.

Morphological data analysis

Phylogenetic analyses were performed using 106 OTUs and a morphological matrix comprising 534 traits, including four outgroups and 11 newly introduced characters (see descriptions and Figs. S1–S12 in Appendix S1, Tables S2 and S3 for details and Appendix S3 for the Tree analysis using New Technology (TNT) file of the matrix). Most traits were compiled and refined from previously published datasets (e.g. Antoine, 2002; Becker et al., 2013; Lu et al., 2023), while 11 were newly created and are described in detail in Appendix S1. Some characters were examined firsthand, but the majority were extracted from the literature. All characters underwent critical review to standardize definitions, states and transformation polarities, with redundant or ambiguous characters removed and additional morphological traits incorporated based on firsthand specimen examination. Furthermore, because many extinct taxa are represented by only a few specimens—sometimes just one—characters originally based on within-taxon frequency have been recorded as simple presence/absence states.

This approach generated an expanded and robust dataset exceeding previous matrices in both character number and quality. A full list of characters, their sources and definitions is provided in Tables S2 and S3. This matrix represents the most comprehensive dataset to date, surpassing previous studies, where the highest number of characters considered was 392 (Lu et al., 2023).

Selected outgroups, treated at the generic level, include *Heptodon* (Tapiroidea), *Hyrachyus* (Rhinocerotoidea), *Hyracodon* (Hyracodontidae) and *Juxia* (Paraceratheriidae). These taxa were chosen based on their antiquity (all are of Eocene age, except *Hyracodon*, which persisted into the Oligocene), their primitiveness relative to the focal clades and the completeness of available material.

Phylogenetic analyses employed three approaches: MP parsimony in TNT v.1.6 (Goloboff and Morales, 2023), ML in IQ-TREE 2.3.4 (Nguyen et al., 2015) and BI in MrBayes 3.2.7a (Ronquist et al., 2012). Calculations in TNT used a script developed by Zhang (2025). Topology constraints were applied in all analyses to align the results with molecular-based phylogenetic hypotheses for Rhinocerotidae. A consensus tree integrating the three methods was obtained in IQ-TREE.

For MP analyses in TNT, heuristic tree searches employed TBR swapping and TNT's search options, including sectorial searches, tree drifting, ratchet and tree fusing, to efficiently explore tree space and identify optimal trees. Parameters included 100 000 replicates with 10 trees saved per replicate. All characters were treated as unordered. Three weighting strategies were tested: equal weighting, implied weighting and extended implied weighting. For implied weighting, the K parameter controlling the downweighting of homoplastic characters was explored from 1 to 50. The optimal K value was selected based on a combined assessment of tree metrics—Consistency Index (CI), Retention Index (RI), Tree Length (TL)—and the degree of resolution and stability of resulting topologies. The best results maximized CI and RI, minimized TL and produced well-resolved clades with high Bremer support. Extended implied weighting at $K = 48$ yielded the most balanced and robust topology. Branch support was assessed using relative Bremer support, jackknifing, BS and symmetric resampling, with 20 000 replicates.

In IQ-TREE, ModelFinder (Kalyaanamoorthy et al., 2017) identified the best-fitting morphological substitution model as MK + FQ + R4 based on BIC. Tree searches applied an extensive NNI optimisation method, starting from 1000 initial parsimony trees with 1000 unsuccessful iterations as stopping criteria and optimizing the top 100 initial parsimony trees using NNI searches. Branch support was assessed using SH-aLRT with 10 000 replicates, as well as non-parametric BS with 2000 replicates.

For BI in MrBayes, a standard discrete morphological model was used, incorporating gamma-distributed rate heterogeneity across sites with five categories. Two independent runs, each with 96 Markov chains, sampled trees every 100 generations over 100 million generations total. The chain heating temperature was set to 0.0001 based on preliminary testing. A posterior consensus tree was generated from trees sampled in the final 31,143 million generations after convergence was confirmed by a stabilized standard deviation of split frequencies well below the recommended threshold of 0.01. ESS values exceeded 200 and PSRF approached 1.0 for all parameters.

Divergence time estimation

Divergence times within Rhinocerotoidea were estimated using BEAST 2.7.6 (Bouckaert et al., 2019), implementing the fossilized birth–death model (Stadler et al., 2018) with topological constraints derived from consensus trees based on combined morphological and molecular datasets. An optimized relaxed clock model was employed alongside an independent Mk model (Lewis, 2001), allowing gamma-distributed rate heterogeneity across sites. Nine character partitions, automatically identified, were assigned five discrete rate categories each. *Heptodon* served as the outgroup.

Model selection through marginal likelihood estimation using path sampling/stepping-stone algorithm (Baele et al., 2012) with eight steps tested combinations of strict, random local and optimized

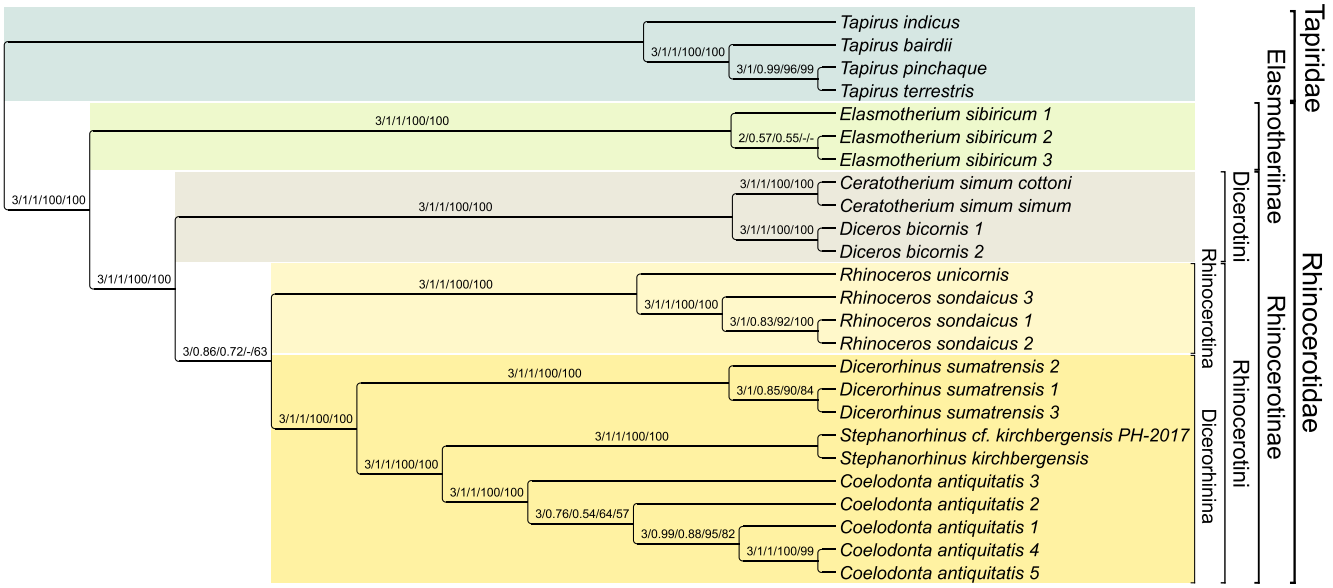

Fig. 1. Phylogenetic consensus tree inferred from mitochondrial genome sequences using three analytical approaches. Node support values are shown in the following order: (1) the number of methods (out of three) supporting each clade; (2) posterior probabilities from MrBayes and PhyloBayes and (3) SH-aLRT and bootstrap support (BS) values from IQ-TREE. Posterior probabilities <0.5 and BS values <50% are omitted or indicated with a dash ('–').

relaxed clock models, alongside substitution models with either equal or gamma-distributed rate variation. The Markov Chain Monte Carlo (MCMC) was run for 100 million generations, with sampling every 500 steps and a 50% burn-in. Calibration assigned tip dates corresponding to minimum occurrence times of taxa, with maximum age modelled as the mean of normal distributions reflecting estimated lineage origins (Table S4) and sigma (standard deviation) set to 1. Other parameters remained at default settings.

Posterior distributions were examined in Tracer 1.7, and all parameters achieved effective sample sizes (ESS) exceeding 200. Convergence and sampling adequacy were confirmed using LogAnalyzer and Tracer. Maximum clade credibility trees were generated in TreeAnnotator, with a 10% burn-in and the assumption of common ancestor node heights. Final trees were visualized using FigTree 1.4.3.

Estimated divergence times displayed strong concordance with the fossil record. Median divergence ages exhibited a high Spearman correlation with the oldest fossil occurrences ($\rho = 0.95$, $P < 2.2e\text{-}16$), and a paired Wilcoxon signed-rank test indicated no significant systematic difference between estimated and fossil-based dates ($P = 0.188$). The median absolute difference was 1.42 Ma; more than 80% of cases fell within 3 Ma of the fossil record, and over 94% within 5 Ma. Most fossil dates were located within or near the 95% Highest Posterior Density (HPD) intervals. In the few instances where fossil dates exceeded the upper HPD bound, the median deviation from the boundary was only 1.15 Ma. These discrepancies are likely attributable to stratigraphic uncertainties associated with fossils lacking direct radiometric age estimates.

Results and discussion

Phylogenetic relationships based on molecular data

To establish a reliable backbone topology for downstream analyses, phylogenetic relationships among rhinocerotid taxa were initially inferred from molecular data, which are generally considered less prone to homoplasy than morphological characters. All three analytical approaches produced a congruent and well-resolved tree, in which the extinct genera *Coelodonta* and *Stephanorhinus* formed a clade sister to extant *Dicerorhinus*, collectively comprising the subtribe Dicerorhinina (Fig. 1). The two extant species of *Rhinoceros* (subtribe Rhinocerotina) were recovered as sister to Dicerorhinina, forming the tribe Rhinocerotini, which in turn is closely related to the tribe Dicerotini, represented by *Ceratotherium* and *Diceros*. These lineages comprise the subfamily Rhinocerotinae, which was recovered as sister to Elasmotheriinae, represented by the extinct genus *Elasmotherium*. Support values were maximal for all major nodes, except for the relationship uniting Dicerorhinina and Rhinocerotina, which received moderate but consistent support across all three analytical methods (Fig. 2). The molecular topology was subsequently employed as a constraint in morphological phylogenetic analyses and divergence time estimation.

The molecular dataset used in this study, representing the most comprehensive to date for Rhinocerotidae, and analysed using advanced probabilistic models, yields robust insights into longstanding taxonomic uncertainties. As previously noted by Willerslev et al. (2009), individual mitochondrial genes often display conflicting phylogenetic signals, a limitation that has affected prior studies. While some mitochondrial-based phylogenies have produced

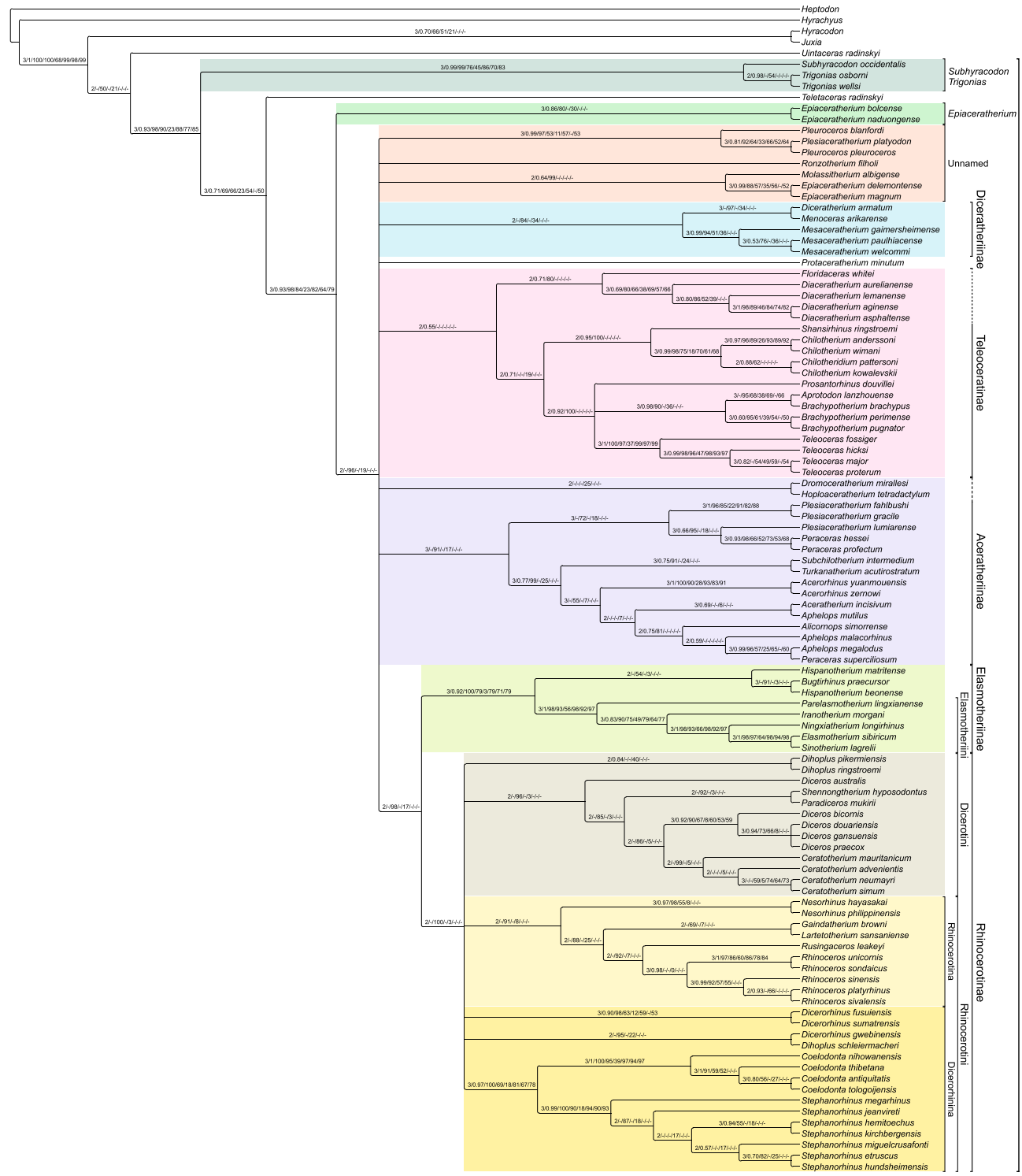

Fig. 2. Phylogenetic consensus tree inferred from morphological character data using three analytical approaches. Clades are colour-coded based on synapomorphies and inferred phylogenetic relationships, including the calibrated tree. Node support values are presented in the following order: (1) number of methods (out of three) supporting each clade; (2) posterior probabilities from MrBayes; (3) SH-aLRT and bootstrap (BS) values from IQ-TREE and (4) relative Bremer support, jackknife, BS and symmetric resampling values from TNT. Posterior probabilities <0.5 and BS values <50% are omitted or represented by a dash ('–').

consistent topologies, others have suggested alternative relationships—for example, *Rhinoceros* more closely related to Dicerotini than to Dicerorhinina (Margaryan et al., 2020), or even questioned the monophyly of *Diceros bicornis* (Stefaniak et al., 2023). Studies by Kirillova et al. (2017), Liu et al. (2021) and Kosintsev et al. (2019) recovered similar topologies, although with fewer taxa and generally lower support values.

Phylogenetic relationships based on morphological data

In contrast to the molecular analyses, the three phylogenetic approaches based on morphological data yielded differing tree topologies. The resulting consensus tree (Fig. 2) resolves relationships among early-diverging taxa, although several later-diverging lineages remain unresolved and appear as polytomies. Nonetheless, multiple clades were consistently recovered by at least two of the methods, including those corresponding to the subfamilies Aceratheriinae, Diceratheriinae and Teleoceratinae, as well as Elasmotheriinae and Rhinocerotinae, which were recovered as sister groups. Within Rhinocerotinae, three distinct clades—Dicerorhinina, Dicerotini and Rhinocerotina—were identified, although their interrelationships remain unresolved. The lack of full congruence across topologies generated by different analytical approaches highlights the need for caution when interpreting results derived from a single method. This methodological inconsistency may also account for conflicting phylogenetic hypotheses reported in previous studies.

The phylogenetic results based on morphological and molecular datasets were subsequently used as topological constraints for estimating the time-calibrated tree (Fig. 3 and Fig. S13). This integrative framework resolves several longstanding systematic and taxonomic uncertainties and recovers a sequence of well-supported clades and evolutionary transitions that correspond closely with major global climatic events discussed in the following sections. Detailed descriptions of synapomorphies defining individual clades are provided in Appendix S1 with associated Fig. S12.

Early-diverging lineages

The phylogenetic placement of key early rhinocerotoid taxa is essential for reconstructing the early evolutionary history of true rhinoceroses. However, previous studies have variably assigned taxa such as *Uintaceras radinskyi*, *Subhyracodon*, *Trigonias* and *Teletaceras* to different positions within Rhinocerotoidea and Rhinocerotidae, reflecting ongoing uncertainty (Bai et al., 2020; Tissier et al., 2020; Deng et al., 2021).

The present analysis consistently recovers *Uintaceras radinskyi* (Fig. 3 and Fig. S13) as an early-diverging member of Rhinocerotoidea, closer to Rhinocerotoidea sensu stricto (Bai et al., 2020) than to Hyracodontidae or Paraceratheriidae. This supports its attribution to Eggysodontidae rather than Rhinocerotidae, based on multiple morphological features (see synapomorphies in Fig. S12 in Appendix S1, as well as Tables S2 and S3 for details), clarifying its previously ambiguous taxonomic status. *Uintaceras* is thus interpreted as a stem lineage within Rhinocerotoidea, distinct from crown rhinocerotids.

The well-supported sister-group relationship between *Subhyracodon* and *Trigonias*—based on shared morphological traits (Appendix S1)—suggests parallel ecological adaptations among Oligocene North American rhinocerotids. This finding helps resolve conflicting phylogenetic hypotheses (Bai et al., 2020; Pandolfi et al., 2021a, b; Antoine et al., 2022; Li et al., 2022, 2024; Uzunidis et al., 2022; Pandolfi, 2023; Pandolfi and Martino, 2024). Along with *Teletaceras*, these taxa likely approximate the ancestral morphotype of Rhinocerotidae.

Teletaceras radinskyi represents a separate lineage that has also been subject to conflicting interpretations. While Tissier et al. (2020) placed it within Rhinocerotidae, Bai et al. (2020) argued for its position as an early-diverging taxon within Rhinocerotoidea, predating the origin of true rhinocerotids. Nonetheless, several morphological features support its inclusion within Rhinocerotidae (Appendix S1).

The monophyly of the genus *Epiaceratherium* is not supported by the results of this study. The Italian species *E. bolcense* and the Vietnamese *E. naduongense* (Tissier et al., 2020) consistently form a sister group and are placed at the base of the derived rhinocerotid clade by all three phylogenetic methods. In contrast, other species traditionally assigned to *Epiaceratherium*, such as the European '*E.*' *delemontense* and '*E.*' *magnum*, instead cluster with early Eurasian rhinoceroses

Fig. 3. Time-calibrated phylogenetic tree (chronogram) based on morphological characters. The colours assigned to the subtrees represent clades defined by synapomorphies and inferred phylogenetic relationships. Drawings of skulls from representative taxa illustrate each clade. Node values indicate the median estimated age along with the 95% Highest Posterior Density (in brackets). The curve under the tree shows variations in global deep-sea oxygen isotope ratios ($\delta^{18}O$), expressed relative to SMOW (Standard Mean Ocean Water) and reflecting long-term trends in global temperature (Zachos et al. 2001). Light red and light blue boxes highlight warm and cold climatic events, respectively: EECO (Early Eocene Climatic Optimum); LTEC-I (Long-term Eocene Cooling I); MECO (Mid-Eocene Climatic Optimum); LTEC-II (Long-term Eocene Cooling II); EOT (Eocene–Oligocene Transition); LOW (Late Oligocene Warming); OMB (Oligocene–Miocene Boundary); MMCO (Mid-Miocene Climatic Optimum); MMCT (Mid-Miocene Climatic Transition) and CT10–4 (Climate Transition between 10 and 4 Ma).

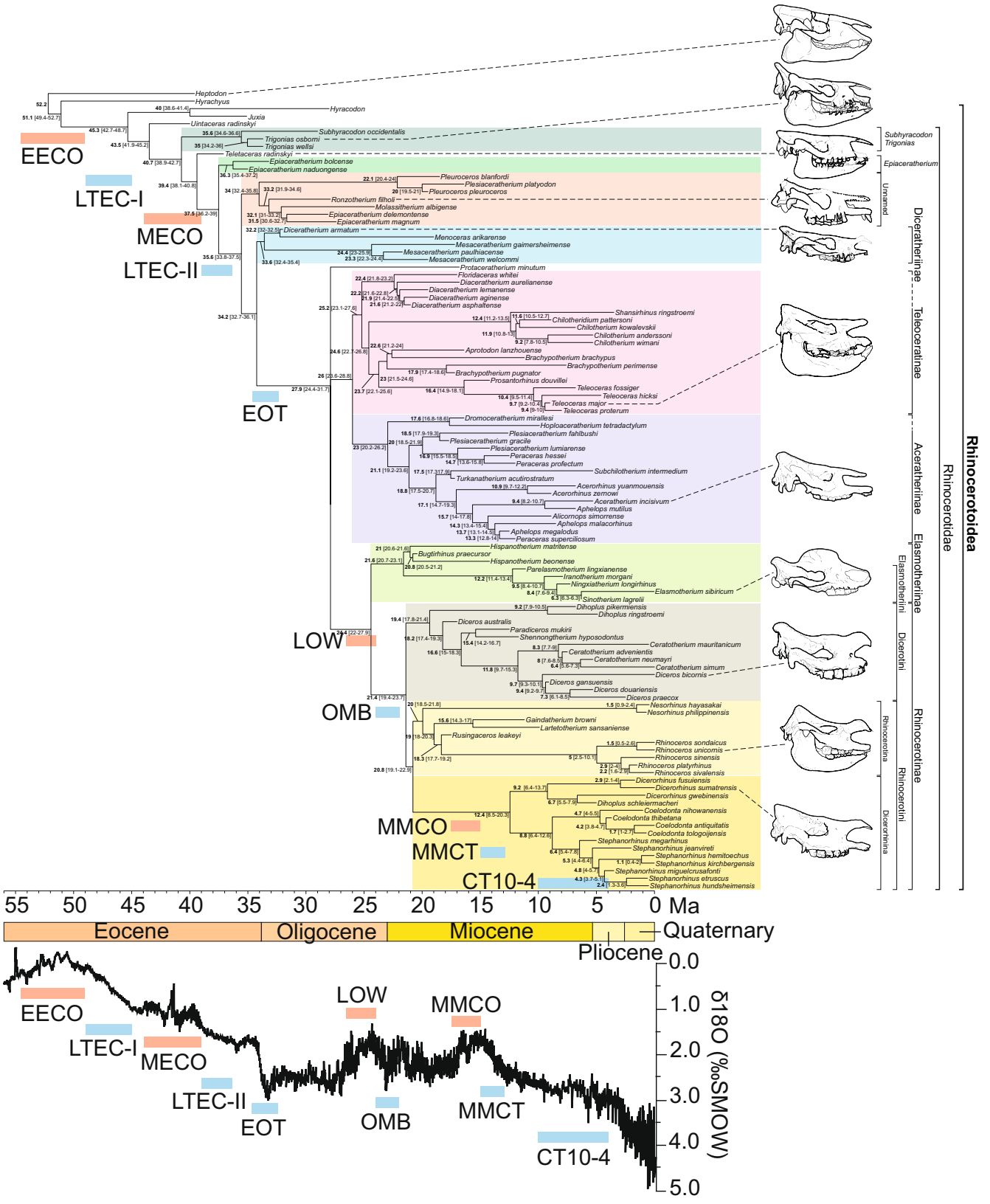

including *Molassitherium* and *Ronzotherium*. This revised circumscription indicates that *Epiaceratherium*, as previously defined, is polyphyletic. Its constituent species represent multiple, independent early rhinocerotid lineages with distinct evolutionary and biogeographic histories.

Overall, this study provides a clearer resolution of the phylogenetic positions of early rhinocerotoid taxa and highlights evolutionary transitions leading to crown Rhinocerotidae. However, persistent uncertainties—particularly regarding highly fragmentary early fossils—underscore the need for additional morphological and molecular data to further refine early rhinocerotid phylogeny.

Diceratheriinae

A well-supported clade comprising *Diceratherium*, *Menoceras* and *Mesaceratherium* is recognized as the subfamily Diceratheriinae, distinguished by a suite of morphological features that set it apart from other early rhinocerotids (Appendix S1). Although previous studies have variably placed *Diceratherium* and *Menoceras*—with some authors positioning them basal to both Rhinocerotinae and Elasmotheriinae (Lu et al., 2023) and others assigning them to Elasmotheriinae (Tissier et al., 2020; Pandolfi et al., 2021a; Li et al., 2022)—the current analyses consistently recover these genera, along with *Mesaceratherium*, as forming a distinct lineage. This lineage appears to be ancestral to the other subfamilies within Rhinocerotidae, highlighting its pivotal role in the early diversification of the group and providing new insights into the macroevolutionary patterns that have shaped rhinocerotid history.

Teleoceratinae and Aceratheriinae

The phylogenetic relationships among the later-diverging subfamilies Teleoceratinae and Aceratheriinae have long been contentious. Some studies have linked Teleoceratinae to Rhinocerotinae (Antoine et al., 2010, 2022; Pandolfi et al., 2021a, b, 2023; Uzunidis et al., 2022; Li et al., 2024; Pandolfi and Martino, 2024) or even to Elasmotheriinae (Antoine et al., 2003), whereas others have proposed closer ties with Aceratheriinae (Tissier et al., 2020; Li et al., 2022; Lu et al., 2023). The calibrated phylogenetic tree presented here supports the last interpretation. This conclusion is reinforced by distinctive synapomorphies, notably a low nasal notch–orbital rim distance relative to skull length and a concave secondary palate.

Additional taxa are newly linked to these subfamilies. In two of the phylogenetic trees, *Floridaceras* and *Diaceratherium* emerge as sister taxa to Teleoceratinae, while the calibrated analysis clusters *Hoploaceratherium* and *Dromoceratherium* with Aceratheriinae—albeit with weak support. *Protaceratherium*, traditionally classified within Aceratheriinae (Roman, 1911; Heissig and Fejfar, 2007), does not show a clear subfamily affiliation in this study.

Teleoceratinae is composed of a diverse array of taxa from Eurasia, Africa and North America, including *Shanshirhinus*, *Chilotherium*, *Aprotodon*, *Brachypotherium*, *Prosantorhinus* and *Teleoceras*, all of which share key derived features (Appendix S1). Although *Chilotherium* and *Shanshirhinus* have frequently been classified within Aceratheriinae/Aceratheres (Antoine et al., 2010; Li et al., 2022; Lu et al., 2023), the present study recovers them as sister taxa within Teleoceratinae in two cladistic analyses. Moreover, *Chilotheridium*, originally described as an independent genus (Hooijer, 1971), is here considered synonymous with *Chilotherium* based on shared derived traits, with *Chilotheridium pattersoni* being more closely related to *Chilotherium kowalevskii* than to other species (Appendix S1).

Consistent with findings by Pandolfi et al. (2021a) and Lu et al. (2023), two analytical approaches support a close relationship between *Shanshirhinus* and *Chilotherium*. Similarly, *Brachypotherium brachypus* consistently clusters with *Aprotodon* across all three trees, sharing several apomorphic features in agreement with Li et al. (2022) (Appendix S1). In contrast, '*Brachypotherium*' *perimense* and '*Brachypotherium*' *pugnator* exhibit closer affinities to one another than to either *Aprotodon* or the type species *Brachypotherium brachypus*, based primarily on dental characteristics (Appendix S1).

The taxonomy of Aceratheriinae remains controversial. Antoine et al. (2010) narrowly defined the clade to include *Chilotherium*, *Aceratherium* and *Alicornops*, whereas broader definitions have included *Protaceratherium*, *Pleuroceros* and *Plesiaceratherium* (= *Dromoceratherium*) *mirallesi*. Similar phylogenies have been recovered by Pandolfi et al. (2021b), Uzunidis et al. (2022), Pandolfi and Martino (2024) and Li et al. (2024). Additional taxa, such as *Hoploaceratherium* (Antoine et al., 2022) and *Plesiaceratherium mirallesi* (Pandolfi, 2023), have also been assigned to this clade. Notably, the phylogenetic tree by Li et al. (2022) expanded the group to include *Chilotherium*, *Aceratherium*, *Alicornops*, *Hoploaceratherium*, *Aphelops*, *Peraceras*, *Acerorhinus* and *Shanshirhinus*, while Lu et al. (2023) further added *Subchilotherium* and *Persiatherium* following Pandolfi et al. (2021a).

In the present study, using three phylogenetic methods, the clade Aceratheriinae is defined to include *Aceratherium*, *Acerorhinus*, *Alicornops*, *Aphelops*, *Peraceras*, *Plesiaceratherium*, *Subchilotherium* and *Turkanatherium*, based on multiple shared synapomorphies (Appendix S1). The analysis focused specifically on

Rhinocerotidae, with only limited sampling of Elasmotheriinae. One of the genera examined, *Turkanatherium*—analysed primarily from the holotype described by Deraniyagala (1951) and more recently by Geraads (2010), as well as from approximately coeval remains from Kenya (Hooijer, 1966, 1967)—was consistently recovered within Aceratheriinae across all analyses, based on the available cranial and dental characters. This placement is consistent with past conclusions (Guérin, 2008), as well as with those of recent studies (e.g. Geraads, 2010). Additional elasmotheriine taxa, such as *Victoriaceros*, were not included due to the scope of the current dataset and the limited availability of comparable morphological data. Future analyses incorporating broader taxon sampling may offer further insights into the affinities of *Turkanatherium* and related taxa.

All three methods employed in this study recover '*Plesiaceratherium*' *lumiarense* as more closely allied with the North American *Peraceras* than with its type species *P. gracile* (Lu et al., 2016), suggesting that '*Plesiaceratherium*' *lumiarense* may belong to a genus more closely related to *Peraceras*, in contrast to the hypothesis of Lu et al. (2023). Furthermore, *Turkanatherium* is consistently recovered not as an Elasmotheriinae but rather as a member of Aceratheriinae, displaying closer affinities to *Subchilotherium* than to other members of the subfamily across all three analyses.

The North American genus *Aphelops* is revealed to be non-monophyletic and exhibits unexpected complexity. All three trees and multiple morphological characters support the grouping of *Aphelops mutilus* with *Aceratherium*, whereas '*Peraceras*' *superciliosum* clusters with the type species, *Aphelops megalodus*, indicating that it should remain within *Aphelops*. Additionally, *Aphelops malacorhinus* is recovered as sister to the latter clade in two of the analyses, sharing the absence of an ectorbital bone as a defining synapomorphy.

Elasmotheriinae and Rhinocerotinae

Recent analyses have suggested a closer affinity between the horned subfamilies Elasmotheriinae and Rhinocerotinae than previously recognised (Lu et al., 2023), contrasting with earlier studies (Antoine et al., 2010; Pandolfi et al., 2021a; Li et al., 2022). In this study, two phylogenetic methods consistently recover shared synapomorphies supporting this revised hypothesis.

Within this framework, Elasmotheriinae is composed of the genera *Bugthirhinus*, *Elasmotherium*, *Hispanotherium*, *Iranotherium*, *Ningxiatherium*, *Parelasmotherium* and *Sinotherium* (Antoine, 2003). This well-supported clade, identified across three phylogenetic approaches, is subdivided into two groups: one comprising *Bugthirhinus* and *Hispanotherium* and the other (Elasmotheriini) containing the remaining genera. Notably, *Hispanotherium beonense* clusters with the more primitive *Bugthirhinus* rather than with *H. matritense*, corroborating its reassignment to the genus *Aegyrcitherium*, as originally proposed by Antoine (1997). The second major clade, which includes the type species *Elasmotherium sibiricum*, is strongly supported across all methods and is defined by distinct cranial, dental and postcranial synapomorphies, such as a well-developed nuchal tubercle, cement-covered cheek teeth and robust limb adaptations (Appendix S1). Contrary to the interpretations of Antoine et al. (2003) and Sun et al. (2023), this study positions *Parelasmotherium* (Deng, 2007) at the base of Elasmotheriinae, alongside *Iranotherium* (Deng, 2005).

The crown group of Rhinocerotidae, encompassing all extant rhinoceroses, has been variably defined in the literature. Some authors refer to this group as Rhinocerotina (Pandolfi et al., 2021a; Uzunidis et al., 2022; Pandolfi, 2023; Pandolfi and Martino, 2024), while others include Aceratheriinae and Teleoceratinae within Rhinocerotinae (Tissier et al., 2020; Antoine et al., 2022; Uzunidis et al., 2022). Moreover, Pandolfi et al. (2021b) incorporated taxa classified as Teleoceratina into Rhinocerotinae. In this study, following the classifications of Li et al. (2024) and Lu et al. (2023), Rhinocerotinae is treated as a distinct subfamily, separate from Aceratheriinae and Teleoceratinae, defined by several synapomorphies (Appendix S1) and supported by two independent cladistic methods.

Within Rhinocerotinae, various clades with differing compositions have been proposed by different authors (e.g. Liu et al., 2021; Pandolfi et al., 2021a, 2022; Antoine et al., 2022; Pandolfi, 2023). Following Liu et al. (2021), this study recognizes two tribes: Dicerotini, which includes extant African species such as *Ceratotherium* and *Diceros*, as well as species such as '*Dihoplus*' *pikermiensis*, '*Dihoplus*' *ringstroemi*, *Paradiceros* and *Shennongtherium* and Rhinocerotini (sensu Liu et al., 2021), comprising genera like *Coelodonta*, *Diceratorhinus*, *Dihoplus*, *Gaindatherium*, *Lartetotherium*, *Nesorhinus*, *Rhinoceros*, *Rusingaceros* and *Stephanorhinus*.

Dicerotini

The present analysis recovers '*Dihoplus*' *pikermiensis* and '*Dihoplus*' *ringstroemi* as early-diverging sister taxa within *Dicerotini*, based on distinctive morphological characters (Appendix S1). Given their phylogenetic position, these species cannot be assigned to *Dihoplus*, the type species of which, *D. schleiermacheri*, is firmly placed within Rhinocerotini. This finding emphasizes the need for a taxonomic revision of these early members of Dicerotini.

The internal composition of *Diceros* and *Ceratotherium* has long been debated due to the shifting assignment of various fossil species. In this study, *Diceros* is clearly diagnosed by several synapomorphies (Appendix S1) and includes *D. bicornis*, *D. douariensis*, *D. gansuensis* and *D. praecox*, forming a well-supported clade across all three phylogenetic approaches. In contrast, '*Diceros*' *australis* is excluded from this clade and not recovered within *Diceros*, likely due to its distinctively more robust Mc II relative to *D. bicornis*, supporting its exclusion from the genus.

The analysis also sheds light on *Paradiceros mukirii*, which emerges as phylogenetically closer to *Shennongtherium hyposodontus* in two trees, united by at least two synapomorphies: a relatively smaller P2 compared to P3–4, and a constriction on the metaloph. *Shennongtherium* remains an enigmatic taxon. Initially described by Huang and Yan (1983) from four isolated teeth and originally referred to Elasmotheriinae, it was later reassigned to Teleoceratina by Antoine et al. (2003). However, this study suggests it represents a derived member of Dicerotini, potentially sister to the *Diceros–Ceratotherium* clade. Nonetheless, its precise phylogenetic position remains tentative due to the fragmentary nature of the available material.

The composition and monophyly of *Ceratotherium* have also been debated, particularly with regard to several Neogene taxa. The results support the distinction of *Ceratotherium* from *Diceros* based on multiple cranial and postcranial traits, with its monophyly confirmed in two of the three phylogenetic analyses. These findings support the inclusion of *Ceratotherium advenientis* within the genus, as previously proposed by Pandolfi et al. (2021a). In contrast to Giaourtsakis (2022), *Ceratotherium neumayri* is not recovered as part of a separate genus (*Miodiceros*), but rather as a valid species within *Ceratotherium*, closely related to *C. simum*, based on results from all three analytical methods and several shared derived features (Appendix S1). The synonymizing of *Ceratotherium mauritanicum* with *C. efficax* has been explicitly rejected by some authors (e.g. Geraads, 2005, 2020). Consistently, the present analyses do not recover it as sister to the *C. neumayri–C. simum* clade. Instead, *C. mauritanicum* occupies a more basal position within *Ceratotherium*, consistent with its distinct morphological features, including more gracile limbs, differences in cranial and horn structure and unique dental traits. These observations support its recognition as a valid and separate taxon, although additional data are required to confirm this placement.

Rhinocerotini

The remaining members of Rhinocerotinae are assigned to the tribe Rhinocerotini, based on a set of shared synapomorphies. This tribe is further divided into two major clades: Rhinocerotina, which includes *Gaindatherium*, *Lartetotherium*, *Nesorhinus*, *Rhinoceros* and *Rusingaceros* and Dicerorhinina, comprising *Coelodonta*, *Dicerorhinus*, *Dihoplus* and *Stephanorhinus*.

The clade Rhinocerotina is well-supported by several synapomorphies (Appendix S1) and is consistently recovered across two phylogenetic methods. Within this clade, the genus *Nesorhinus* is confirmed as monophyletic, supported by shared traits between its two species, and forms a sister group to the remaining Rhinocerotina. Other genera within Rhinocerotina show a closer relationship to *Rhinoceros*, a pattern confirmed by both morphological and phylogenetic evidence.

The genus *Rhinoceros* itself is characterized by several synapomorphies (Appendix S1) and is confirmed as monophyletic across all three phylogenetic methods. Two strongly supported clades are identified: one consisting solely of extant species (*R. unicornis* and *R. sondaicus*) and the other composed exclusively of extinct species (*R. sinensis*, *R. platyrhinus* and *R. sivalensis*). These two clades are distinguished by multiple synapomorphies, particularly in the extant lineage. Based on this evidence, it is proposed to divide the genus into two subgenera: *Rhinoceros* (*Rhinoceros*) for the extant species and *Rhinoceros* (*Punjabitherium*) for the extinct clade.

The second major clade, Dicerorhinina, is united by a series of synapomorphies that distinguish it from Rhinocerotina. Dicerorhinina consists of two primary groups: (1) *Dihoplus* and *Dicerorhinus* and (2) *Coelodonta* and *Stephanorhinus*.

Dicerorhinus has traditionally been considered closely related to *Rhinoceros* (Pandolfi et al., 2021b; Antoine et al., 2022; Pandolfi, 2023; Li et al., 2024; Pandolfi and Martino, 2024). However, the present analysis demonstrates that *Dicerorhinus* is more closely related to *Dihoplus*, based on several synapomorphies (Appendix S1). To a lesser extent, it also shares a closer relationship with *Coelodonta* and *Stephanorhinus*, which aligns with previous studies (Liu et al., 2021; Pandolfi et al., 2021a; Li et al., 2022; Uzunidis et al., 2022).

The genus *Dicerorhinus* is restricted to the type species *Dicerorhinus sumatrensis* and the extinct *D. fusuiensis*, with *D. cixianensis* potentially belonging to this genus, though it was excluded from this analysis due to the fragmentary juvenile specimen available. Notably, *Dicerorhinus gwebinensis* is here reassigned to the genus *Dihoplus*, based on the support of two phylogenetic trees and shared synapomorphies with the type species *Dihoplus schleiermacheri* (Appendix S1).

This analysis also reinforces the close relationship between *Coelodonta* and *Stephanorhinus*, a connection previously suggested by several authors (e.g. Liu et al., 2021; Li et al., 2022, 2024; Uzunidis et al., 2022; Lu et al., 2023; Pandolfi, 2023). This relationship is strongly supported by synapomorphies and is

consistently reflected by high support values across three trees. However, contrary to recent proposals (Cappellini et al., 2019), *Coelodonta* is not included within the genus *Stephanorhinus*. Both genera remain monophyletic across all three approaches, each distinguished by several synapomorphies (Appendix S1).

Recent studies have suggested that *Stephanorhinus miguelcrusafonti* and *Dihoplus megarhinus* (originally described as *Rhinoceros megarhinus* and later assigned to *Dicerorhinus* and subsequently *Stephanorhinus* by de Christol, 1834; Mottl, 1939; Kretzoi, 1942; Thenius, 1955; Fortelius et al., 1993; Giaourtsakis, 2003) may belong to a newly established genus, *Pliorhinus* (Pandolfi et al., 2021b; Pandolfi, 2023; Li et al., 2024; Pandolfi and Martino, 2024). However, the present study finds that *Pliorhinus* is no longer supported as a monophyletic genus. Instead, *Pliorhinus megarhinus* is placed at the base of *Stephanorhinus*, while *Pliorhinus miguelcrusafonti* is embedded within *Stephanorhinus*, potentially at the base of a clade containing *Stephanorhinus etruscus* and *S. hundsheimensis*. Consequently, *Pliorhinus* is synonymized with *Stephanorhinus*, with *S. megarhinus* regarded as one of the least derived species in this group, alongside *S. jeanvireti*. Additionally, *Stephanorhinus kirchbergensis* and *S. hemitoechus* are found to be closely related in all three trees, based on multiple traits.

Although *S. kirchbergensis* and *S. megarhinus* share notable similarities in dental and metapodial morphology (e.g. Fortelius et al., 1993), recent comprehensive phylogenetic analyses suggest that these traits are more likely the result of convergent evolution than of close common ancestry (e.g. Pandolfi et al., 2021b; Li et al., 2024). Consistent with previous studies, *S. kirchbergensis* is recovered as the sister taxon to *S. hemitoechus*, while *S. megarhinus* occupies a more basal position within the genus *Stephanorhinus*. This topology is supported by a broad set of cranial, dental and postcranial characters, indicating that the traditional hypothesis of a clade comprising *S. megarhinus* and *S. kirchbergensis* is not supported by the total evidence. Although some superficially similar morphological features may appear shared by the two species in the character matrix, the broader dataset yields a stronger and more reliable phylogenetic signal.

Finally, *Stephanorhinus miguelcrusafonti* may be more closely related to *S. etruscus* and *S. hundsheimensis*, although this hypothesis is supported by a relatively limited number of dental characters and only two of the cladistic methods employed.

Evolutionary history and ecological adaptations of major Rhinocerotoidea clades

The well-resolved, time-calibrated phylogenetic tree presented in this study provides a robust framework for synthesizing rhinocerotoid evolutionary history within a temporal context, integrating patterns of diversification, biogeography and ecological change with major climatic and environmental changes. This framework facilitates the exploration of how environmental pressures, lineage-specific constraints and stochastic processes have shaped rhinocerotoid evolutionary trajectories. Rather than adopting overly simplistic adaptationist narratives, the study embraces the complexity of evolutionary responses and emphasizes the formulation of testable hypotheses grounded in morphological and paleoecological evidence (Zachos et al., 2001; Mudelsee et al., 2014; Pandolfi, 2018; Bai et al., 2020).

Divergence and early evolution in the Eocene and Oligocene

The initial divergence and early diversification of rhinocerotoids appear closely linked to the geological and climatic transformations of the Paleogene. The divergence between Tapiroidea and Rhinocerotoidea is estimated at approximately 53–46 Ma, with the stem Rhinocerotoidea dating to approximately 57–52 Ma (Bai et al., 2020). This interval coincided with significant geotectonic and climatic events, including global temperature fluctuations (Zachos et al., 2001; Mudelsee et al., 2014) and major paleogeographic reorganisations, such as the collision of the Indian subcontinent with Asia (Hu et al., 2016) and the rifting between Europe and North America (~55–53 Ma: Buiter et al., 2023), which occurred at the transition from the Palaeocene-Eocene Thermal Maximum (PETM) to the Early Eocene Climatic Optimum (EECO: Mudelsee et al., 2014). These events likely influenced early rhinocerotoid dispersal and ecological diversification by reshaping habitats and corridors, as reflected in the early branches of the calibrated phylogeny (Fig. 3).

Stem Rinocerotidae diverged from other rhinocerotoids around 45–42 Ma, with early rhinocerotid diversification occurring between 43 and 39 Ma during the initial uplift of the Southern and Central Tibetan Plateau (Tada et al., 2016) and the Middle Eocene Climatic Optimum (MECO), which temporarily interrupted the Long-term Eocene Cooling Phases I and II (LTEC-I and LTEC-II: Zachos et al., 2001; Mudelsee et al., 2014). Early lineages, such as *Subhyracodon* and *Trigonias*, exhibited ecological differentiation: *Subhyracodon* shows cursorial limb adaptations consistent with more open habitats, while *Trigonias* retained graviportal limb morphology suited to mixed woodland environments (Prothero, 2005; Pandolfi, 2018). These morphological differences illustrate early ecological partitioning within Rhinocerotidae, likely influenced but not solely determined by climatic trends, with potential roles for phylogenetic constraints and habitat heterogeneity.

Between approximately 39 and 34 Ma, rhinocerotoid diversification intensified, particularly in Europe, coinciding with the Late Eocene Cooling and the Eocene–Oligocene Transition (EOT: Mudelsee et al., 2014). During this interval, the common ancestor of four major subfamilies—Teleoceratinae, Aceratheriinae, Elasmotheriinae and Rhinocerotinae—emerged. The genus *Epiaceratherium*, which originated around 36 Ma in either Europe or South Asia, exemplifies early Europe-Asia transcontinental dispersal events likely facilitated by sea level regressions and changing land connections (Antoine et al., 2003; Bai et al., 2020). Species such as *Teletaceras borissiaki* adapted morphologically to transitional environments, while representatives of *Ronzotherium*, *Epiaceratherium*, *Plesiaceratherium* and *Pleuroceros* occupied temperate to subtropical habitats, demonstrating notable dietary flexibility inferred from dental morphology and microwear analyses (Fortelius et al., 2003, 2014; Wang and Secord, 2020). This dietary flexibility may have facilitated survival during fluctuating climatic regimes, although the extent to which it reflects active adaptation versus pre-existing ecological breadth remains unresolved.

The emergence of the subfamily Diceratheriinae during this period, characterized by morphological adaptations to open plains and sparsely wooded habitats, including limb proportions favouring cursorial locomotion and dentition suited to a mixed diet of fibrous grasses and browsing foliage, further illustrates the interplay between climate-driven habitat shifts and morphological evolution (Prothero, 2005; Pandolfi, 2018). By 32 Ma, Diceratheriinae had dispersed into North America under cooler climatic conditions, which may reflect both environmental pressures and biogeographic opportunities.

Late Oligocene and Miocene radiations and extinctions

The major diversification events and extinctions of rhinocerotids during the Oligocene and Miocene epochs can also be linked with climatic and environmental changes. The common ancestor of the remaining subfamilies of Rhinocerotidae likely existed between 32 and 24 Ma, coinciding with the Late Oligocene Warming (LOW: 26.5–24 Ma). The Teleoceratinae diversified between 28 and 23 Ma, primarily in Europe or north-central Asia, inhabiting riparian and wetland habitats. Genera such as *Prosantorhinus* and *Teleoceras* developed robust dentition adapted to processing fibrous vegetation, consistent with isotopic evidence for mixed feeding (Fortelius et al., 2014). The Aceratheriinae radiated slightly later, between 26 and 20 Ma, exhibiting broad ecological flexibility that allowed them to occupy woodlands, riparian zones and open habitats, as inferred from morphological diversity and paleoenvironmental reconstructions (Agustí et al., 1997; Fortelius et al., 2003; Pandolfi, 2018). These radiations coincided with the Oligocene–Miocene Boundary (OMB), a period marked by climatic fluctuations including a transient glaciation, which likely influenced habitat availability and connectivity.

Relatively rapid climate fluctuations—the warm Mid-Miocene Climatic Optimum (MMCO, 17–15 Ma) followed by the colder Middle Miocene Climate Transition (MMCT, 15–13 Ma)—further influenced the diversification of rhinocerotid subfamilies. During this period, members of the Aceratheriinae expanded into North America. In the late Miocene (ca. 7–5 Ma), C4 grasslands began to spread globally (Cerling et al., 1993), and some genera, such as *Teleoceras* exhibited adaptations to these new vegetation types, as indicated by dental morphology and stable isotope data (MacFadden, 1998). However, both Teleoceratinae and Aceratheriinae became extinct during the Climate Transition at 10–4 Ma (CT10–4), likely due to increasing aridification and cooling temperatures that reduced warm, subtropical habitats and favoured open, dry landscapes dominated by tough vegetation (Prothero, 2005; Pandolfi, 2018). These extinctions highlight the complex and sometimes lineage-specific responses of rhinocerotids to long-term climatic change, emphasizing that extinction risk is modulated by multiple factors including ecological specialisation and geographic range.

Later evolved subfamilies

The diversification and ecological adaptations of the most recent groups, Elasmotheriinae and Rhinocerotinae, occurred after the extinction of other major lineages, Teleoceratinae and Aceratheriinae, and show a strong correlation with Neogene climatic shifts. The common ancestor of Elasmotheriinae and Rhinocerotinae likely appeared between 28 and 22 Ma during the Late Oligocene Warming (LOW). Their diversification began in Europe between 24 and 19 Ma, during the cold Oligocene–Miocene Boundary (OMB), a relatively cool period marked by episodic Antarctic glaciation and the uplift of the Tibetan Plateau (Agustí et al., 1997; Tada et al., 2016), and continued through MMCO and MMCT. The diversification then accelerated in the Late Miocene, driven by progressive global cooling and the expansion of C4 grasslands associated with the Climate Transition (CT10–4), which fostered adaptations to increasingly diverse environments and feeding strategies (Agustí et al., 1997, 1999; Pandolfi, 2018). These evolutionary patterns mirror broader ecological trends observed in large herbivores across different continents, demonstrating the influence of climatic events on megafaunal diversification.

Elasmotheriinae evolved into large-bodied grazers adapted to steppe-like environments dominated by fibrous vegetation, with grazing adaptations initiating in the middle to late Early Miocene, well before the Late Miocene climatic events (Kahlke, 1999, 2014; Antoine, 2002). This protracted evolutionary trend underscores the importance of long-term climatic and environmental factors rather than singular events in shaping morphology and ecology.

Dietary and habitat adaptations within Rhinocerotinae exhibit considerable heterogeneity. For example, one genus of the tribe Dicerotini, *Ceratotherium*, shows a well-documented trend towards increased grazing, supported by dental morphology and stable isotope analyses (Hernesniemi et al., 2011; Pandolfi, 2018), whereas the other, *Diceros*, remained predominantly a browser, consistent with its conserved dental and cranial morphology (Hernesniemi et al., 2011). Even within the sole extant genus of Rhinocerotina (*Rhinoceros*), *R. sondaicus*, with brachyodont molars, has remained a browser, whereas *R. unicornis*, with mesodont molars, has evolved towards mixed feeding (Taylor et al., 2013). This dietary differentiation likely reflects ecological niche partitioning rather than uniform clade-wide adaptation.

Similarly, *Dicerorhinus* (Dicerorhinina) has maintained relatively conservative morphology and low-level browsing strategies in dense woodlands and grasslands, suggesting evolutionary constraints and ecological stability over time despite environmental fluctuations (Pandolfi, 2018). However, divergence between other genera within Dicerorhinina—namely *Coelodonta* and *Stephanorhinus*—is estimated to have occurred between 13 and 6 Ma, with subsequent species diversification between 8 and 0.4 Ma. These evolutionary patterns may reflect responses to climatic and environmental changes occurring during the CT10–4 interval (Kahlke, 1999; Antoine, 2002).

Climatic aridification and cooling during the Messinian (6–5.3 Ma) prompted rhinocerotid migration and radiations in Africa and North America, leading to the emergence of new taxa adapted to cold, open environments. Extreme adaptations to cold, open environments evolved independently in Elasmotheriinae and Rhinocerotinae, as exemplified by *Elasmotherium* and *Coelodonta*. These genera developed traits such as thick hair coats and highly specialized dentitions. In *Elasmotherium*, the molars were rootless and ever-growing (hypselodont), while *Coelodonta* exhibited hypsodont molars with increased crown height and thick coronal cement—a condition known as plagiolophodonty in *Coelodonta*. These specialized molar morphologies, strongly associated with grazing, enabled efficient processing of abrasive grasses and fibrous vegetation typical of steppe environments (Kahlke, 1999, 2014; Antoine, 2002; Prothero, 2005; Deng et al., 2011; Fortelius et al., 2014; Wang, 2016; Pandolfi, 2018; Wang and Secord, 2020).

Overall, the evolutionary history of rhinocerotoids reflects a complex interplay of climatic change, geographic dispersal, ecological opportunity and lineage-specific constraints. Morphological adaptations, dietary shifts and habitat preferences evolved over protracted timescales and varied among clades, underscoring the importance of integrating phylogenetic, paleoecological and paleoclimatic data to understand megafaunal macroevolution.

Conclusions

This study demonstrates the effectiveness of an integrative framework combining morphological, molecular, fossil and paleoclimatic data to reconstruct the evolutionary history of Rhinocerotidae. A robust backbone topology, derived from molecular data, served as a constraint for phylogenetic analyses based on an expanded morphological dataset, enabling the inclusion of numerous extinct taxa. Although the analytical approaches applied to this combined dataset yielded some topological discrepancies, the resulting consensus tree recovered several well-supported clades, including both early-diverging and more derived clades. Time-calibrated analyses, informed by fossil constraints, resolved previously ambiguous relationships and provided a framework for reevaluating long-standing systematic and taxonomic issues. The phylogenetic and temporal structure recovered here clarifies the origins and early diversification of Rhinocerotidae, supporting a North American origin in the Late Eocene (Chadronian, ~37–34 Ma), followed by dispersal into Eurasia at the Eocene–Oligocene transition (~34 Ma). This dispersal into Europe triggered a major diversification event, ultimately giving rise to five subfamilies. Aceratheriinae and Teoleoceratinae likely originated from a common European ancestor and subsequently dispersed back into North America, as evidenced by Miocene fossils such as *Aphelops* and *Peraceras*. Meanwhile, Elasmotheriinae and Rhinocerotinae evolved in Europe and Africa from around 25 Ma, replacing earlier lineages adapted to warm, subtropical climates and instead thriving in open habitats and cooler climates. The expansion of grasslands in the Late Miocene played a pivotal role in their diversification, driving dental adaptations in grazing taxa. Morphological changes, particularly in cranial and dental structures, underscore the evolutionary impact of dietary specialisation. This multidisciplinary and comprehensive study provides a solid foundation for future research into the evolutionary history of Rhinocerotidae.

Acknowledgements

The authors thank Stefano Dominici, Luca Bellucci and Andrea Savorelli for granting access to the rhinoceros remains housed in the Paleontology Section, Museum of Natural History, University of Florence. This is important to include, as it supports our statement in the paper that we directly examined the specimens. AB thanks superintendent Alessandro Betori (Soprintendenza Archeologia, Belle Arti e Paesaggio per le Province di Frosinone e Latina). We are also grateful to Michael Fortelius, Emmanuel M.E. Billia and the anonymous reviewer, whose insightful comments and suggestions greatly improved this work. P.P.A.M. was supported in the present study by PAULMAZZARI-CATEN24—Mazza P. Fondo Ateneo 2024 MUR (the Italian Ministry of Universities and Research) grant. The study was supported by a subsidy 2025; (501); MPK 2599280000 ZP; discipline 73 granted to K.S. and U.R.-S. Some computations were carried out at the Wrocław Centre for Networking and Supercomputing (Grant No. 307), granted to P.M.

[Corrections added on 7 November 2025, after first online publication: the Acknowledgement section has been updated in this version.]

Conflict of interest

The authors declare no competing interests.

Data availability statement

The authors declare that the other data supporting the findings of this study are available within the paper and its Supporting Information files.

References

Agustí, J., Cabrera, L., Garces, M. and Parés, J.M., 1997. The Vallesian mammal succession in the Vallès-Penedès basin (northeast Spain): paleomagnetic calibration and correlation with global events. Palaeogeogr. Palaeoclimatol. Palaeoecol. 133, 149–180.

Agustí, J., Cabrera, L., Garcés, M. and Llenas, M., 1999. Mammal turnover and global climate change in the late Miocene terrestrial record of the Vallès-Penedès Basin (NE Spain). In: Agustí, J., Rook, L. and Andrews, P. (Eds.), Hominoid Evolution and Climatic Change in Europe. Cambridge University Press, Cambridge, UK, pp. 397–412.

Antoine, P.O., 1997. *Aegyrcitherium beonensis* n.g. n. sp., nouvel élasmothère (Mammalia, Rhinocerotidae) du gisement miocène (MN 4b) de Montréal-du-Gers (Gers, France). Position phylogénétique au sein des Elasmotheriini. Neues Jahrb. Geol. Palaeontol. Abh. 204, 399–414.

Antoine, P.O., 2002. Phylogenie et evolution des Elasmotheriina (Mammalia, Rhinocerotidae). Mém. Mus. Natl. Hist. Nat. Paris 188, 1–353.

Antoine, P.O., 2003. Middle Miocene elasmotheriine (Rhinocerotidae) from China and Mongolia: taxonomic revision and phylogenetic relationships. Zool. Scr. 32, 95–118.

Antoine, P.O., Downing, K.F., Crochet, J.Y., Duranthon, F., Flynn, L.J., Marivaux, L., Métais, G., Rajpar, A.R. and Roohi, G., 2010. A revision of *Aceratherium blanfordi* Lydekker, 1884 (Mammalia: Rhinocerotidae) from the Early Miocene of Pakistan: postcranials as a key. Zool. J. Linnean Soc. 160, 139–194.

Antoine, P.O., Duranthon, F. and Welcomme, J.L., 2003. *Alicornops* (Mammalia, Rhinocerotidae) dans le Miocène supérieur des collines Bugti (Balouchistan, Pakistan): implications phylogénétiques. Geodiversitas 25, 575–603.

Antoine, P.O., Reyes, M.C., Amano, N., Bautista, A.P., Chang, C.H., Claude, J., De Vos, J. and Ingicco, T., 2022. A new rhinoceros clade from the Pleistocene of Asia sheds light on mammal dispersals to the Philippines. Zool. J. Linnean Soc. 194, 416–430.

Baele, G., Lemey, P., Bedford, T., Rambaut, A., Suchard, M.A. and Alekseyenko, A.V., 2012. Improving the accuracy of demographic and molecular clock model comparison while accommodating phylogenetic uncertainty. Mol. Biol. Evol. 29, 2157–2167.

Bai, B., Meng, J., Zhang, C., Gong, Y.X. and Wang, Y.Q., 2020. The origin of Rhinocerotoidea and phylogeny of Ceratomorpha (Mammalia, Perissodactyla). Commun. Biol. 3, 509.

Becker, D., Antoine, P.O. and Maridet, O., 2013. A new genus of Rhinocerotidae (Mammalia, Perissodactyla) from the Oligocene of Europe. J. Syst. Palaeontol. 11, 947–972.

Bouckaert, R., Vaughan, T.G., Barido-Sottani, J., Duchêne, S., Fourment, M., Gavryushkina, A., Heled, J., Jones, G., Kühnert, D., de Maio, N., Matschiner, M., Mendes, F.K., Müller, N.F., Ogilvie, H.A., du Plessis, L., Popinga, A., Rambaut, A., Rasmussen, D., Siveroni, I., Suchard, M.A., Wu, C.H., Xie, D., Zhang, C., Stadler, T. and Drummond, A.J., 2019. BEAST 2.5: an advanced software platform for Bayesian evolutionary analysis. PLoS Comput. Biol. 15, e1006650.

Buiter, S.J., Brune, S., Keir, D. and Peron-Pinvidic, G., 2023. Rifting continents. In: Dynamics of Plate Tectonics and Mantle Convection, 1st edition. Elsevier, Amsterdam, Netherlands, pp. 459–481.

Cappellini, E., Welker, F., Pandolfi, L., Ramos-Madrigal, J., Samodova, D., Rüther, P.L., Fotakis, A.K., Lyon, D., Moreno-Mayar, J.V., Bukhsianidze, M., Rakownikow Jersie-Christensen, R., Mackie, M., Ginolhac, A., Ferring, R., Tappen, M., Palkopoulou, E., Dickinson, M.R., Stafford, T.W., Chan, Y.L., Götherström, A., Nathan, S.K.S.S., Heintzman, P.D., Kapp, J.D., Kirillova, I., Moodley, Y., Agusti, J., Kahlke, R.-D., Kiladze, G., Martínez-Navarro, B., Liu, S., Sandoval Velasco, M., Sinding, M.-H.S., Kelstrup, C.D., Allentoft, M.E., Orlando, L., Penkman, K., Shapiro, B., Rook, L., Dalén, L., Gilbert, M.T.P., Olsen, J.V., Lordkipanidze, D. and Willerslev, E., 2019. Early Pleistocene enamel proteome from Dmanisi resolves *Stephanorhinus* phylogeny. Nature 574, 103–107.

Cerling, T.E., Wang, Y. and Quade, J., 1993. Expansion of C4 ecosystems as an indicator of global ecological change in the late Miocene. Nature 361, 344–345.

Chernomor, O., von Haeseler, A. and Minh, B.Q., 2016. Terrace aware data structure for phylogenomic inference from supermatrices. Syst. Biol. 65, 997–1008.

Christol, J.D., 1834. Recherches sur les Grandes Espèces de Rhinocéros Fossiles. J. Martel, Montpellier.

Deng, T., 2005. New discovery of *Iranotherium morgani* (Perissodactyla, Rhinocerotidae) from the late Miocene of the Linxia Basin in Gansu, China, and its sexual dimorphism. J. Vertebr. Paleontol. 25, 442–450.

Deng, T., 2007. Skull of *Parelasmotherium* (Perissodactyla, Rhinocerotidae) from the upper Miocene in the Linxia Basin (Gansu, China). J. Vertebr. Paleontol. 27, 467–475.

Deng, T., Lu, X., Wang, S., Flynn, L.J., Sun, D., He, W. and Chen, S., 2021. An Oligocene giant rhino provides insights into *Paraceratherium* evolution. Commun. Biol. 4, 639.

Deng, T., Wang, X., Fortelius, M., Li, Q., Wang, Y., Tseng, Z.J., Takeuchi, G.T., Saylor, J.E., Säilä, L.K. and Xie, G., 2011. Out of Tibet: Pliocene woolly rhino suggests high-plateau origin of Ice Age megaherbivores. Science 333, 1285–1288.

Deraniyagala, P.E.P., 1951. A hornless rhinoceros from the Mio-Pliocene deposits of East Africa. Spolia Zeylanica 26, 133–135.

Fortelius, M., Eronen, J.T., Kaya, F., Tang, H., Raia, P. and Puolmäki, K., 2014. Evolution of Neogene mammals in Eurasia: environmental forcing and biotic interactions. Annu. Rev. Earth Planet. Sci. 42, 579–604.

Fortelius, M., Heissig, K., Sarac, G. and Sen, S., 2003. Rhinocerotidae (Perissodactyla). In: Fortelius, M., Kappelman, J.W., Sen, S. and Bernor, R.L. (Eds.), Geology and Paleontology of the Miocene Sinap Formation, Turkey. Columbia University Press, New York City, USA, pp. 282–307.

Fortelius, M., Mazza, P. and Sala, B., 1993. *Stephanorhinus* (Mammalia: Rhinocerotidae) of the western European Pleistocene, with a revision of *S. etruscus* (Falconer, 1868). Palaeontogr. Ital. 80, 63–155.

Geraads, D., 2005. Pliocene Rhinocerotidae (Mammalia) from Hadar and Dikika (Lower Awash, Ethiopia), and a revision of the origin of modern African rhinos. J. Vertebr. Paleontol. 25, 451–461.

Geraads, D., 2010. Rhinocerotidae. In: Werdelin, L. and Sanders, W.J. (Eds.), Cenozoic Mammals of Africa. University of California Press, Berkeley, pp. 675–689.

Geraads, D., 2020. Perissodactyla (Rhinocerotidae and Equidae) from Kanapoi. J. Hum. Evol. 140, 102373.

Giaourtsakis, I.X., 2003. Late Neogene Rhinocerotidae of Greece: distribution, diversity and stratigraphical range. Deinsea 10, 235–254.

Giaourtsakis, I.X., 2022. The fossil record of rhinocerotids (Mammalia: Perissodactyla: Rhinocerotidae) in Greece. In: Fossil Vertebrates of Greece. Vol. 2: Laurasiatherians, Artiodactyles, Perissodactyles, Carnivorans, and Island Endemics. Springer, Cham, Switzerland, pp. 409–500.

Goloboff, P.A. and Morales, M.E., 2023. TNT version 1.6, with a graphical interface for MacOS and Linux, including new routines in parallel. Cladistics 39, 144–153.

Groves, C.P., 1983. Phylogeny of the living species of rhinoceros. J. Zool. Syst. Evol. Res. 21, 293–313.

Groves, C.P., 1997. Die Nashörner: Stammesgeschichte und Verwandtschaft. In: Ganslosser, U. (Ed.), Nashörner: Begegnung mit Urzetliche Kolossen. Filander Verlag, Fürth, Germany, pp. 14–32.

Guérin, C., 1980. Les rhinoceros (Mammalia, Perissodactyla) du Miocene terminal au Pleistocene superieur en Europe occidentale; comparaison avec les especes actuelles. Doc. Lab. Géol. Fac. Sci. Lyon 79, 3–1183.

Guérin, C., 2008. The Miocene Rhinocerotidae (Mammalia) of the Northern Sperrgebiet, Namibia. Memoir of the Geological Survey of Namibia 20, 331–341.

Heissig, K., 1973. Die Unterfamilien und Tribus der rezenten und fossilen Rhinocerotidae (Mammalia). Säugetierkd. Mitt. 21, 25–30.

Heissig, K., 1996. The stratigraphic range of fossil rhinoceroses in the Late Neogene of Europe and the Eastern Mediterranean. In: Bernor, R.L., Fahlbusch, V.L. and Mittman, H.-W. (Eds.), The Evolution of Western Eurasian Neogene Mammal Faunas. Columbia University Press, New York City, USA, pp. 339–347.

Heissig, K. and Fejfar, O., 2007. Die fossilen Nashörner (Mammalia, Rhinocerotidae) aus dem Untermiozän von Tuchorice in Nordwestböhmen. Sborník Národního Muzea v Praze (Acta Musei Nat. Pragae B) 63, 19–64.

Hernesniemi, E., Blomstedt, K. and Fortelius, M., 2011. Multi-view stereo three-dimensional reconstruction of lower molars of recent and Pleistocene rhinoceroses for mesowear analysis. Palaeontol. Electron. 14(2), 2T.

Hooijer, D.A., 1966. Fossil mammals of Africa, no. 21. Miocene rhinoceroses of East Africa. Bulletin of the British Museum (Natural History), Geology 13, 119–190.

Hooijer, D.A., 1967. The status of *Aceratherium Leakei* Deraniyagala. Zoologische Mededelingen 42, 121–123.

Hooijer, D.A., 1971. A new rhinoceros from the Late Miocene of Loperot, Turkana district, Kenya. Bull. Mus. Comp. Zool. Harv. Univ. 142, 339–392.

Hu, X., Garzanti, E., Wang, J., Huang, W., An, W. and Webb, A., 2016. The timing of India-Asia collision onset–facts, theories, controversies. Earth-Sci. Rev. 160, 264–299.

Huang, W. and Yan, D., 1983. New material of Elasmotherini from Shennongjia, Hubei. Vertebr. PalAsiat. 21, 223–229.

Huelsenbeck, J.P., Larget, B. and Alfaro, M.E., 2004. Bayesian phylogenetic model selection using reversible jump Markov chain Monte Carlo. Mol. Biol. Evol. 21, 1123–1133.

Kahlke, R.-D., 1999. The History of the Origin, Evolution and Dispersal of the Late Pleistocene *Mammuthus–Coelodonta* Faunal Complex in Eurasia (Large Mammals). The Mammoth Site of Hot Springs, South Dakota, Inc., Bypass, Hot Springs, SD 57747, United States.

Kahlke, R.D., 2014. The origin of Eurasian mammoth faunas (*Mammuthus–Coelodonta* Faunal Complex). Quat. Sci. Rev. 96, 32–49.

Kalyaanamoorthy, S., Minh, B.Q., Wong, T.K., Von Haeseler, A. and Jermiin, L.S., 2017. ModelFinder: fast model selection for accurate phylogenetic estimates. Nat. Methods 14, 587–589.

Kampouridis, P., Hartung, J., Ferreira, G.S. and Böhme, M., 2021. Reappraisal of the late Miocene elasmotheriine *Parelasmotherium schansiense* from Kutschwan (Shanxi Province, China) and its phylogenetic relationships. J. Vertebr. Paleontol. 41, e2080556.

Katoh, K. and Standley, D.M., 2013. MAFFT multiple sequence alignment software version 7: improvements in performance and usability. Mol. Biol. Evol. 30, 772–780.

Kirillova, I.V., Chernova, O.F., Van der Made, J., Kukarskih, V.V., Shapiro, B., van der Plicht, J., Shidlovskiy, F.K., Heintzmann, P.D., van Kolfschoten, O. and Zanina, O.G., 2017. Discovery of the skull of *Stephanorhinus kirchbergensis* (Jäger, 1839) above the Arctic Circle. Quat. Res. 88, 537–550.

Kosintsev, P., Mitchell, K.J., Devièse, T., Van der Plicht, J., Kuitems, M., Petrova, E., Tikhonov, A., Higham, T., Comeskey, D., Turney, C., Cooper, A., van Kolfschoten, T., Stuart, A.J. and Lister, A.M., 2019. Evolution and extinction of the giant rhinoceros *Elasmotherium sibiricum* sheds light on late Quaternary megafaunal extinctions. Nat. Ecol. Evol. 3, 31–38.

Kretzoi, M., 1942. Bemerkungen zum System der nachmiozänen Nashorn-Gattungen. Földt. Közl. 72, 309–318.

Lacombat, F., 2006. Morphological and biometrical differentiation of the teeth from Pleistocene species of *Stephanorhinus* (Mammalia, Perissodactyla, Rhinocerotidae) in Mediterranean Europe and the Massif Central, France. Palaeontogr. Abt. A 274, 71–111.

Lartillot, N. and Philippe, H., 2004. A Bayesian mixture model for across-site heterogeneities in the amino-acid replacement process. Mol. Biol. Evol. 21, 1095–1109.

Lewis, P.O., 2001. A likelihood approach to estimating phylogeny from discrete morphological character data. Syst. Biol. 50, 913–925.

Li, S., Jiangzuo, Q. and Deng, T., 2022. Body mass of the giant rhinos (Paraceratheriinae, Mammalia) and its tendency in evolution. Hist. Biol. 56, 1–12.

Li, S., Sanisidro, O., Wang, S., Yang, R. and Deng, T., 2024. New materials of *Pliorhinus ringstroemi* from the Linxia Basin (Late Miocene, eastern Asia) and their taxonomical and evolutionary implications. J. Mamm. Evol. 31, 6.

Liu, S., Westbury, M.V., Dussex, N., Mitchell, K.J., Sinding, M.H.S., Heintzman, P.D., Duchêne, D.A., Kapp, J.D., von Seth, J., Heiniger, H., Sánchez-Barreiro, F., Margaryan, A., André-Olsen, R., De Cahsan, B., Meng, G., Yang, C., Chen, L., van der Valk, T., Moodley, Y., Rookmaker, K., Bruford, M.W., Ryder, O., Steiner, C., Bruins-van Sonsbeek, L.G.R., Vartanyan, S., Guo, C., Cooper, A., Kosintey, P., Kirillova, I., Lister, A.M., Marques-Bonet, T., Gopalakrishnan, S., Dunn, R.R., Lorenzen, E.D., Shapiro, B., Zhang, G., Antoine, P.-O., Dalén, L. and Gilbert, M.T.P., 2021.

Ancient and modern genomes unravel the evolutionary history of the rhinoceros family. Cell 184, 4874–4885.
Lord, E., Pathmanathan, J.S., Corel, E., Makarenkov, V., Lopez, P., Bouchard, F. and Bapteste, E., 2019. Introducing trait networks to elucidate the fluidity of organismal evolution using palaeontological data. Genome Biol. Evol. 11, 2653–2665.
Lu, X., Zheng, X., Sullivan, C. and Tan, J., 2016. A skull of *Plesiaceratherium gracile* (Rhinocerotidae, Perissodactyla) from a new lower Miocene locality in Shandong Province, China, and the phylogenetic position of *Plesiaceratherium*. J. Vertebr. Paleontol. 36, e1095201.
Lu, X.K., Deng, T. and Pandolfi, L., 2023. Reconstructing the phylogeny of the hornless rhinoceros Aceratheriinae. Front. Ecol. Evol. 11, 1005126.
MacFadden, B.J., 1998. Tale of two rhinos: isotopic ecology, paleodiet, and niche differentiation of *Aphelops* and *Teleoceras* from the Florida Neogene. Paleobiology 24, 274–286.
Margaryan, A., Sinding, M.H.S., Liu, S., Vieira, F.G., Chan, Y.L., Nathan, S.K., Moodley, Y., Bruford, M.W. and Gilbert, M.T.P., 2020. Recent mitochondrial lineage extinction in the critically endangered Javan rhinoceros. Zool. J. Linnean Soc. 190, 372–383.
McKenna, M.C. and Bell, S.K., 1997. Classification of Mammals: Above the Species Level. Columbia University Press, New York City, USA.
Moodley, Y., Westbury, M.V., Russo, I.R.M., Gopalakrishnan, S., Rakotoarivelo, A., Olsen, R.A., Prost, S., Tunstall, T., Ryder, O.A., Dalén, L. and Bruford, M.W., 2020. Interspecific gene flow and the evolution of specialization in black and white rhinoceros. Mol. Biol. Evol. 37, 3105–3117.
Mottl, M., 1939. Die mittelpliozäne Säugetierfauna von Gödöllö bei Budapest. Jahrb. Ungar. Geol. Anst. 32, 257–350.
Mudelsee, M., Bickert, T., Lear, C.H. and Lohmann, G., 2014. Cenozoic climate changes: A review based on time series analysis of marine benthic $\delta^{18}O$ records. Rev. Geophys. 52, 333–374.
Nguyen, L.T., Schmidt, H.A., Von Haeseler, A. and Minh, B.Q., 2015. IQ-TREE: a fast and effective stochastic algorithm for estimating maximum-likelihood phylogenies. Mol. Biol. Evol. 32, 268–274.
Pandolfi, L., 2018. Evolutionary history of Rhinocerotina (Mammalia, Perissodactyla). Fossilia 2018, 27–32.
Pandolfi, L., 2023. Reassessing the phylogeny of Quaternary Eurasian Rhinocerotidae. J. Quat. Sci. 38, 291–294.
Pandolfi, L., Marra, A.C., Carone, G., Maiorino, L. and Rook, L., 2021a. A new rhinocerotid (Mammalia, Rhinocerotidae) from the latest Miocene of Southern Italy. Hist. Biol. 33, 194–208.
Pandolfi, L. and Martino, R., 2024. Taxonomy and phylogeny of the smallest Miocene rhinocerotid *Parvorhinus* n. gen. (Mammalia, Rhinocerotidae). Palaeoworld 33, 229–240.
Pandolfi, L., Martino, R. and Palombo, M.R., 2023. New insights on the fossil mammals from Casal de'Pazzi (Rome). J. Mediterr. Earth Sci. 15, 1–19.
Pandolfi, L., Pierre-Olivier, A., Bukhsianidze, M., Lordkipanidze, D. and Rook, L., 2021b. Northern Eurasian rhinocerotines (Mammalia, Perissodactyla) by the Pliocene–Pleistocene transition: phylogeny and historical biogeography. J. Syst. Palaeontol. 19, 1031–1057.
Pandolfi, L., Sendra, J., Reolid, M. and Rook, L., 2022. New Pliocene Rhinocerotidae findings from the Iberian Peninsula and the revision of the Spanish Pliocene records. PalZ 96, 343–354.
Piras, P., Maiorino, L., Raia, P., Marcolini, F., Salvi, D., Vignoli, L. and Kotsakis, T., 2010. Functional and phylogenetic constraints in Rhinocerotinae craniodental morphology. Evol. Ecol. Res. 12, 897–928.
Prothero, D.R., 1998. Rhinocerotidae. In: Evolution of Tertiary Mammals of North America, Cambridge University Press, Cambridge, UK, p. 595.
Prothero, D.R., 2005. The Evolution of North American Rhinoceroses. Cambridge University Press, Cambridge, UK.
Prothero, D.R., Guerin, C. and Manning, E., 1989. 16. The history of the Rhinocerotoidea. In: Prothero, D.R. and Schoch, R.M. (Eds.), The Evolution of Perissodactyls, Vol. 15. Oxford University Press, Oxford, UK, pp. 321–340.
Prothero, D.R., Manning, E. and Hanson, C.B., 1986. The phylogeny of the Rhinocerotoidea (Mammalia, Perissodactyla). Zool. J. Linnean Soc. 87, 341–366.
Prothero, D.R. and Schoch, R.M., 2002. Horns, Tusks, and Flippers: The Evolution of Hoofed Mammals.John Hopkins University Press, Baltimore, Maryland, USA.
Roman, M.F., 1911. Les Rhinocérotidés de l'Oligocène d'Europe. Arch. Mus. Hist. Nat. Lyon 11, 1–92.
Ronquist, F., Teslenko, M., van der Mark, P., Ayres, D.L., Darling, A., Hohna, S., Larget, B., Liu, L., Suchard, M.A. and Huelsenbeck, J.P., 2012. MrBayes 3.2: efficient Bayesian phylogenetic inference and model choice across a large model space. Syst. Biol. 61, 539–542.
Saarinen, J., 2019. The palaeontology of browsing and grazing. In: The Ecology of Browsing and Grazing, Vol. 2. Springer, New York City, USA, pp. 5–59.
Stadler, T., Gavryushkina, A., Warnock, R.C., Drummond, A.J. and Heath, T.A., 2018. The fossilized birth-death model for the analysis of stratigraphic range data under different speciation modes. J. Theor. Biol. 447, 41–55.
Stefaniak, K., Kotowski, A., Badura, J., Sobczyk, A., Borówka, R.K., Stachowicz-Rybka, R., Moskal-del Hoyo, M., Hrynowiecka, A., Tomkowiak, J., Sławińska, J., Przybylski, B., Ciszek, D., Alexandrowicz, W.P., Skoczylas-Śniaz, S., Ratajczak-Skrzatek, U., Shpansky, A.V., Ilyina, S.A., Moska, P., Urbański, K., Mirosław-Grabowska, J., Niska, M., Capalbo, C., Nowakowski, D., van der Made, J., Popović, D., Baca, M. and Billia, E.M.E., 2023. A skeleton of peat-trapped forest rhinoceros *Stephanorhinus kirchbergensis* (Jäger, 1839) from Gorzów Wielkopolski, Northwestern Poland: a record of life and death of the Eemian large mammals. Neues Jahrb. Geol. Palaontol. Abh. 308, 45–77.
Sun, D., Deng, T., Lu, X. and Wang, S., 2023. A new elasmothere genus and species from the middle Miocene of Tongxin, Ningxia, China, and its phylogenetic relationship. J. Syst. Palaeontol. 21, 2236619.
Tada, R., Zheng, H. and Clift, P.D., 2016. Evolution and variability of the Asian monsoon and its potential linkage with uplift of the Himalaya and Tibetan Plateau. Prog Earth Planet Sci 3, 1–26.
Taylor, L.A., Kaiser, T.M., Schwitzer, C., Müller, D.W., Codron, D., Clauss, M. and Schulz, E., 2013. Detecting inter-cusp and inter-tooth wear patterns in Rhinocerotids. PLoS One 8, e80921.
Thenius, E., 1955. Die Verknöcherung der Nasenscheidewand bei Rhinocerotiden und ihr Systematischer Wert: zum Geschlechtsdimorphismus Fossiler Rhinocerotiden. Birkhäuser, Basel, Switzerland.
Tissier, J., Antoine, P.O. and Becker, D., 2020. New material of *Epiaceratherium* and a new species of *Mesaceratherium* clear up the phylogeny of early Rhinocerotidae (Perissodactyla). R. Soc. Open Sci. 7, 200633.
Tissier, J., Antoine, P.O. and Becker, D., 2021. New species, revision, and phylogeny of *Ronzotherium* Aymard, 1854 (Perissodactyla, Rhinocerotidae). Eur. J. Taxon. 753, 1–80.
Uzunidis, A., Antoine, P.O. and Brugal, J.P., 2022. A middle Pleistocene *Coelodonta antiquitatis praecursor* (Mammalia, Perissodactyla) from Les Rameaux, SW France, and a revised phylogeny of Coelodonta. Quat. Sci. Rev. 288, 107594.
Wang, B., 2016. Reconstructing the paleoecology and biogeography of rhinoceroses (Mammalia: Rhinocerotidae) in the Great Plains of North America, leading up to their extinction in the Early Pliocene. M.S. Thesis. Department of Earth and Atmospheric Sciences, University of Nebraska-Lincoln.
Wang, B. and Secord, R., 2020. Paleoecology of *Aphelops* and *Teleoceras* (Rhinocerotidae) through an interval of changing climate and vegetation in the Neogene of the Great Plains, central United States. Palaeogeogr. Palaeoclimatol. Palaeoecol. 542, 109411.
Waterhouse, A.M., Procter, J.B., Martin, D.M., Clamp, M. and Barton, G.J., 2009. Jalview version 2—a multiple sequence

alignment editor and analysis workbench. Bioinformatics 25, 1189–1191.
Willerslev, E., Gilbert, M.T., Binladen, J., Ho, S.Y., Campos, P.F., Ratan, A., Tomsho, L.P., da Fonseca, R.R., Sher, A., Kuznetsova, T.V., Nowak-Kemp, M., Roth, T.L., Miller, W. and Schuster, S.C., 2009. Analysis of complete mitochondrial genomes from extinct and extant rhinoceroses reveals lack of phylogenetic resolution. BMC Evol. Biol. 9, 1–11.
Zachos, J., Pagani, M., Sloan, L., Thomas, E. and Billups, K., 2001. Trends, rhythms, and aberrations in global climate 65 Ma to present. Science 292, 686–693.
Zhang, G., 2025. guoyi. run: one-step TNT script for maximum parsimony phylogenetic analysis. Zootaxa 5642, 96–98.

Supporting Information

Additional supporting information may be found online in the Supporting Information section at the end of the article.

Appendix S1. List of morphological characters.
Fig. S1. Character 96.
Fig. S2. Character 120.
Fig. S3. Character 124.
Fig. S4. Character 127.
Fig. S5. Character 147.
Fig. S6. Character 154.
Fig. S7. Character 246.
Fig. S8. Character 277.
Fig. S9. Character 372.
Fig. S10. Character 388.
Fig. S11. Character 525.
Fig. S12. Phylogenetic tree of Rhinocerotidae based on a combined analysis of molecular and morphological characters.
Fig. S13. Calibrated phylogenetic tree (chronogram) based on morphological characters and molecular constraints.
Appendix S2. Nexus file containing the alignment of 37 concatenated mitochondrial sequences, including protein-coding genes, RNA genes and noncoding regions from rhinoceroses and tapirs.
Appendix S3. TNT file containing the morphological character matrix for rhinoceroses and related taxa.
Table S1. GenBank accession numbers of mitochondrial genomes used in the study.
Table S2. Morphological character matrix used in the study.
Table S3. Topology and character states for molar hypsodonty.
Table S4. Characteristics of studied taxa; references.